ISSN 0915-633X

NATIONAL INSTITUTE FOR FUSION SCIENCE

Free-Boundary Equilibrium Studies for the Large Helical Device

H.J. Gardner and K. Ichiguchi

(Received – June 1, 1993)

NIFS-231 June 1993

RESEARCH REPORT
NIFS Series

NAGOYA, JAPAN

Free-Boundary Equilibrium Studies for the Large Helical Device

H.J. Gardner* and K. Ichiguchi,
National Institute for Fusion Science,
Nagoya 464-01, Japan

Permanent Address:
Plasma Research Laboratory and Department of Theoretical Physics,
Research School of Physical Sciences and Engineering,
Australian National University,
Canberra, ACT 0200,
Australia

Abstract

A free-boundary version of the VMEC three-dimensional equilibrium code, together with a code, DIAGNO, to determine the response to a set of magnetic diagnostic coils has been applied to the Large Helical Device. Two sequences of equilibria were considered: one where an external vertical field was used to keep the plasma centered and another where the outwardly shifting plasma was truncated by a limiter. The predictions of a simple cylindrical model have been verified for a diamagnetic loop. A set of simple response curves has been obtained which should be useful for the analysis and control of the finite $<\beta>$ plasma. The ideal Mercier criterion suggests that the centered plasma might be more stable.

Keywords Large Helical Device, free boundary, VMEC, magnetic diagnostics, diamagnetic flux, plasma control

1. Background

Of the three-dimensional magnetohydrodynamic equilibrium codes employed in fusion research, the most widely used is the Variational Moments Equilibrium Code, VMEC [1]. A free-bounday version of VMEC [2] has been written which incorporates a Green's function method for calculating the magnetic field in the vacuum region due to the plasma currents alone (originally implemented as the NESTOR code[3]).

An obvious application of a model for the fields outside of a magnetically-confined plasma due to the plasma currents alone is the design and analysis of magnetic diagnostics: flux loops, pick-up coils and Rogowski coils. This sort of modelling is routinely carried out for tokamaks. In the three-dimensional case, NESTOR was used as a basis for constructing the DIAGNO code [4,5], a post-processor for the free-boundary version of VMEC to calculate the expected signals of the magnetic diagnostics on the Wendelstein 7AS stellarator [5,6]. Some of these results have subsequently been compared with experiment with good agreement [7].

In the present study, we describe the results of an adaptation of the DIAGNO code to model, in combination with VMEC, the Large Helical Device (LHD). The equilibrium sequences, and diagnostic arrays, chosen are intended to demonstrate the codes rather than to suggest an optimal experimental arrangement for LHD. Some of the issues involved in the stability of LHD free-boundary equilibria to ideal Mercier modes will also be discussed.

2. Methodology

The model system comprises a standard model for the vacuum magnetic field of LHD, an additional, constant, vertical "B_z" field to control the plasma position and a limiter. The diagnostic system is composed of a diamagnetic loop in the plane of the vertical ellipse and four pick-up coils in the plane of the horizontal ellipse. The vertical limiter is on the outboard side of the machine in the plane of the horizontal ellipse.

For a fixed pressure profile, $p(s) \propto (1-s)^2$, where s is the normalised flux, free-boundary equilibria were calculated for plasma $<\beta>$'s between 0 and 3%. The limiter condition, $R_{max} = 4.49$ metres, was enforced in two different ways. In "Sequence 1" equilibria the total toroidal flux, Ψ_b, inside the plasma was held constant and B_z was adjusted to satisfy the limiter condition. In "Sequence 2" equilibria, B_z was set to zero and the total plasma flux was reduced to elliminate surfaces which had passed to the

outboard side of the limiter with increasing $<\beta>$. In both cases the choice of B_z, or total flux, at a specific $<\beta>$ had to be found by experimentation and the results below have an error of less than 0.5 cm for R_{max}.

VMEC was run with a maximum poloidal mode number of 7 (mpol=8) and maximum toroidal mode number of 8. The angular grid was set to 32×32 and an initial radial grid of 11 surfaces was interpolated to 33 surfaces for the main iteration. The energy minimisation was usually terminated when the parameter monitoring the square of the residual forces, "ftol", reached $1. \times 10^{-11}$. The accuracy of the free-boundary part of the algorithm was monitored by the relative jump in the magnetic pressure across the final plasma surface which was of the order of $5. \times 10^{-4}$. The major exception to these conditions was the 3% $<\beta>$ case of Sequence 2 which converged to an ftol of the order of 10^{-9} with an error at the boundary of $1. \times 10^{-3}$. The low $<\beta>$ cases generally took about half an hour, and the high-beta cases one hour, on the Fujitsu vp2200 at the Australian National University. In some circumstances this can be reduced by using a "restart" version of the free-boundary code [5] to change the parameters of an already converged equilibrium.

In its fixed-boundary mode, VMEC usually runs with Ψ_b equal to π [8]. The results presented here used MKS units throughout, which meant that the plasma volume could be shrunk by decreasing Ψ_b directly without invoking an extra "curpol" scaling factor as is sometimes done.

Figure 1 compares the vacuum rotational transforms for both fixed boundary and free boundary equilibrium runs. The horizontal scale gives the radial distance from the center of the torus in the plane of the vertical ellipse. The agreement between the two is excellent.

3. Results: Sequence 1 and Sequence 2

When the total plasma flux is held constant the additional vertical field needed to satisfy the limiter condition is shown in Fig. 2. Figures 3 and 4 show the plasma bounday in the planes of the vertical and horizontal ellipses for $<\beta>$ of 0.14% and 2.73%. The solid line in Fig. 3 designates the diamagnetic loop. The limiter and the pick-up coils are shown in Fig. 4.

The simple theory for a cylindrical theta pinch predicts that the diamagnetic flux excluded by a plasma should be given by

$$\Phi_{\mathrm{dia}} = -\frac{<\beta>}{2}\Psi_b \qquad (1)$$

where Ψ_b is the total toroidal flux. Pustovitov [9] has calculated the corrections to this result for conventional stellarators similar to LHD and has found them to be small. (We note, however, that numerical evidence has been presented that the measured diamagnetic signals in the Wendelstein 7AS stellarator might depend on the geometry of the diamagnetic loops with respect to the plasma surface [5].)

The results of Fig. 5 appear to be an excellent verification of the theoretical prediction: if Ψ_b is held constant then Φ_{dia} varies linearly with $<\beta>$. Figure 6 shows one component (in the "poloidal" direction) of the magnetic field at each of the pick-up coils (numbering in from the outboard side). All of the results of Figs. 5 and 6 extrapolate uniformly to zero at zero $<\beta>$ which is another verification that the free-boundary equilibria are accurate.

Figures 7 and 8 show the boundary contours for equilibria of Sequence 2 at $<\beta>$'s of 0.14% and 3.04%. The decrease in Ψ_b with $<\beta>$ causes the diagnostic signals shown in Figs. 9 and 10 to level out. As would be expected, the pick-up coils on the outboard side are more sensitive to changes in the plasma pressure in this case.

4. Discussion

A hypothetical control sequence for an LHD discharge might start with an estimate of the plasma $<\beta>$, based on the heating power used, and read a value of B_z from Fig. 2 which would keep the plasma approximately centered. Figure 2 and the curves for Sequence 1 assume that the total plasma flux is known beforehand which is not the case in a real experiment (although it may *approximately* be the case if the plasma remains centered). On the other hand the vertical field and limiter position are well-known external parameters, so that the actual $<\beta>$ *and the total flux* could be read from curves of the type of Sequence 2. The vertical field could then be iterated using curves similar to Fig. 2. Although the flatness of some of the curves of Sequence 2 could make it difficult to determine $<\beta>$, this should not be a problem if the plasma is kept reasonably centered to start with. Alternatively, greater reliance could be put on pick-up coils on the outboard side. The magnitude of the field due to the plasma curents at $<\beta> = 3\%$ is about two orders of magnitude less than the main toroidal field and should be experimentally measurable.

The major sources of error in this study are the accuracy of the equilibrium solution and the accuracy of the Green's function integration over the plasma surface to evaluate the diagnostic signals. Both of these factors may

contribute to the slight deviation of the calculated value for the $<\beta> = 3\%$ case of Sequence 2 from the theoretical curve.

5. Mercier Stability

A portrait of the ideal Mercier stability of fixed-boundary LHD equilibria, with and without secondary currents, has been presented in Ref. [10]. An interesting question in relation to the present study is whether the the increased magnetic well resulting from the free-boundary Shafranov shift will stabilise the equilibria of Sequence 2 with respect to Sequence 1.

Figures 11 and 12 show the results of the JMC Mercier stability code[11] for Sequences 1 and 2 at $<\beta> = 2.7\%$ and 3% respectively. The three terms correspond to the "well" (D_w) "parallel current" (D_g) and total ideal Mercier criterion (D_i) of Ref. [12] except that the scaling factors involving π and ι have been dropped and the complete expression has been multiplied by s^2 as advocated in Ref. [13]. This means that the first term in the criterion is equal to $s^2\iota'^2/4$ in contrast to the usual unscaled criterion[10] where it is $\iota'^2/4$. This scaling by s^2 makes D_i dimensionless so that its values at different flux surfaces can be compared without becoming singular at the magnetic axis (as is the case with the unscaled criterion) or when $\iota' = 0$ (as is the case with the usual dimensionless form where $D_i = 1/4 + \ldots$). (The shear term, which is not plotted, is the difference between D_i and $D_w + D_g$.) The plasma is Mercier stable if $D_i > 0$. The parallel currents in the Mercier criterion have been calculated after transforming to Boozer coordinates with 30 modes in the poloidal and 20 modes in the toroidal direction. Although the transformation is made with this full matrix of modes, the summation to calculate the parallel current is only carried out for poloidal mode numbers less than 15 with the justification that higher order islands will occur with a localised flattening of the pressure profile with only a small effect on the overall plasma $<\beta>$.

Figure 11, for the centered equilibria, is, perhaps, a more conventional picture of the moderate-beta bahaviour of LHD. The maximum magnetic well over-compenstates for the maximum destabilising parallel current which occurs near the turning point in the ι profile. Closer to the boundary there is significant shear stabilisation. The plasma is stable at all values of s. The Sequence 2 case of Fig. 12 is unstable near the turning point in ι due to the dominant contributions of harmonics of the parallel current with the toroidal mode numbers equal to zero (which are resonant with $\iota = 0$). In this case, the poorer convergence of VMEC and the cramped nature of the

ι profile in real space (see Figs. 13 and 14) make it possible that the plasma may have exceeded its "equilibrium limit".

6. Conclusion

This study opens the door for a more detailed examination of the possibilities of magnetic diagnostics on the Large Helical Device. Further work should examine the optimal location of any pick-up coils with a view to verifying the symmetry of the plasma currents as well as determining any possible variation with respect to internal plasma pressure and current profiles (although we remark that the profile dependence found in earlier studies [5,15] appeared to be weak). One early application of this modelling might also be to the diamagnetic measurements on the CHS stellarator, although we recall that, for the diamagnetic loop chosen, the simple, cylindrical theory appears to be very accurate [9].

The free-bounday equilibria appear to be sufficiently accurate to enable a diagnostic system to be modelled in the way described in this paper. A logical extension to the free-boundary VMEC code would be to implement the limiter condition in a self-consistent manner which could be done using the "Sequence 2" equilibria (with MKS scaling) as an example: Once an almost converged equilibrium is found then the change in Ψ_b needed to extend or reduce the limit of the plasma boundary could be estimated by interpolation or extrapolation of the values of Ψ_b within the plasma. The case of separatrix-limited plasmas might be handled by monitoring the change in the direction of the radius of curvature of the plasma boundary near where it attempts to push through the separatrix (Fig. 15).

The results of the Mercier stability study show that centered equilibria are likely to be more stable (as well as physically larger). The simple, linear relationship between the vertical field needed to achieve this and the plasma $<\beta>$ shown in Fig. 2 should be useful for the feed-back control of the LHD plasma.

Acknowledgements

H.J. Gardner wishes to thank the staff of the National Institute for Fusion Science for their hospitality during the time that he spent there as a Visiting Professor. He also acknowledges the Japanese Ministry of Science, Education and Culture, Monbusho, for their financial support. Both authors wish to thank Professor M. Okamoto for his encouragement. The computations were performed on the Fujitsu vp2200 at the Australian National University Supercomputer Facility.

References

1. HIRSHMAN, S.P., WHITSON, J.C., Phys. Fluids **26** (1983) 3553.
2. HIRSHMAN, S.P., VAN RIJ, W.I., MERKEL, P., Comput. Phys. Commun. **43** (1986) 143.
3. MERKEL, P., J. Comput. Phys. **66** (1986) 83.
4. MERKEL, P., in Theory of Fusion Plasmas (Proc. Workshop Varenna, 1988), CEC, Brussels (1988) 25.
5. GARDNER, H.J., Nucl. Fus. **30** (1990) 1417.
6. RITTGER, E., Max Planck Institute for Plasma Physics report IPP 2/314 (1992).
7. RENNER, H. in Proc. 19th Eur. Phys. Soc. Conf. Innsbruck, (1992).
8. HIRSHMAN, S.P., LEE, D.K., Comput. Phys. Commun. **39** (1986) 161.
9. PUSTOVITOV, V.D., National Institute for Fusion Science report NIFS-162 (1992)
10. ICHIGUCHI, K., *et al.*, Nucl. Fusion **33** (1993) 481.
11. NÜHRENBERG, J., ZILLE, R., in Proc. 5th Int. Workshop on Stellarators, Vol. 1, CEC, Brussels (1984) 339.
12. BAUER, F., BETANCOURT, O., GARABEDIAN, P., Magnetohydrodynamic Equilibrium and Stability of Stellarators, Springer-Verlag, Berlin, New York (1984).

13. GARABEDIAN, P., SIAM Rev. **31** (1989) 542.

14. GARDNER, H.J., BLACKWELL, B.D., Nucl. Fus. **32** (1992) 2009.

15. MORRIS, R.N., *et al.* Nucl. Fus. **29** (1989) 2115.

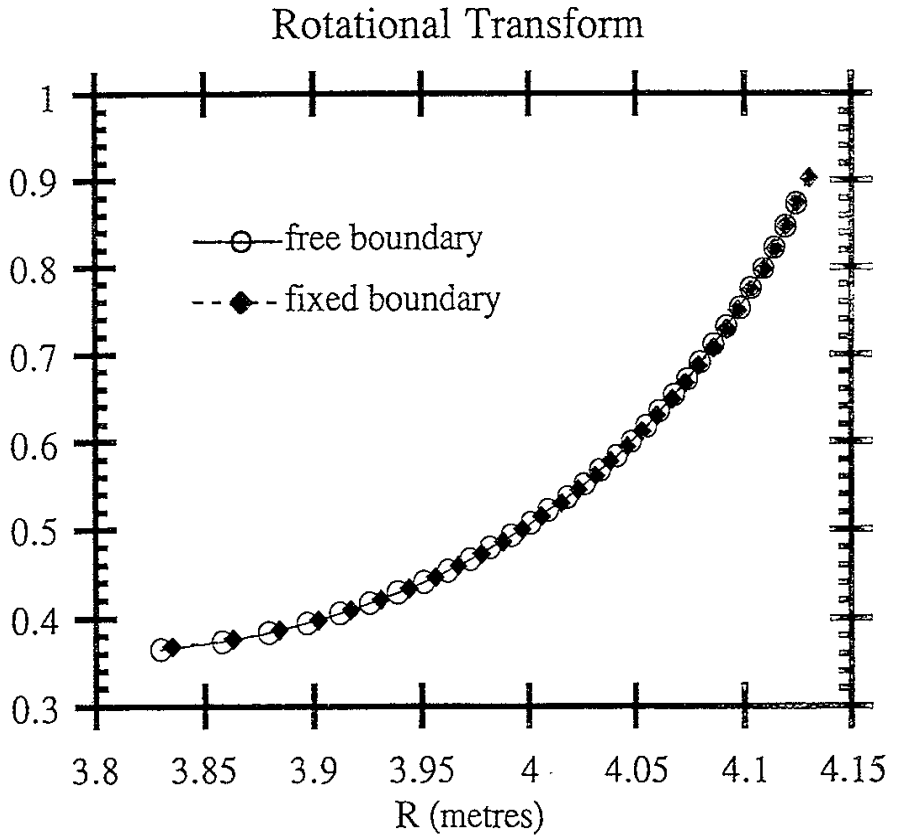

Figure 1: Comparison of the rotational transform profiles of fixed and free boundary vacuum calculations for LHD. The transforms are plotted against the major radius in the plane of the vertical ellipse.

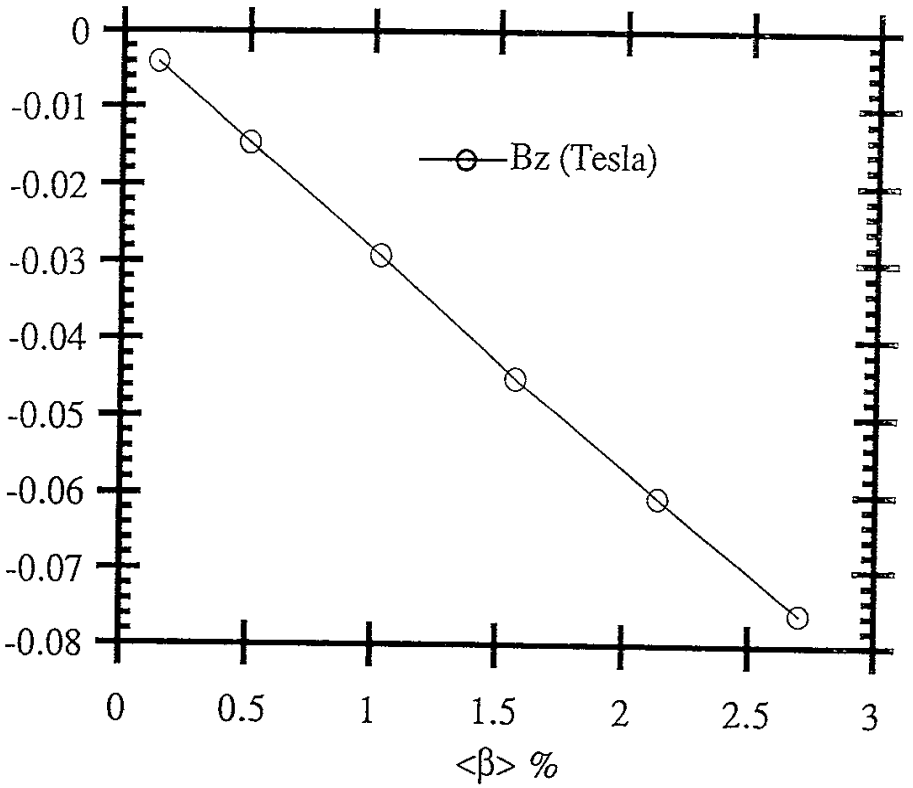

Figure 2: The extra vertical field needed to satisfy the limiter condition for Sequence 1.

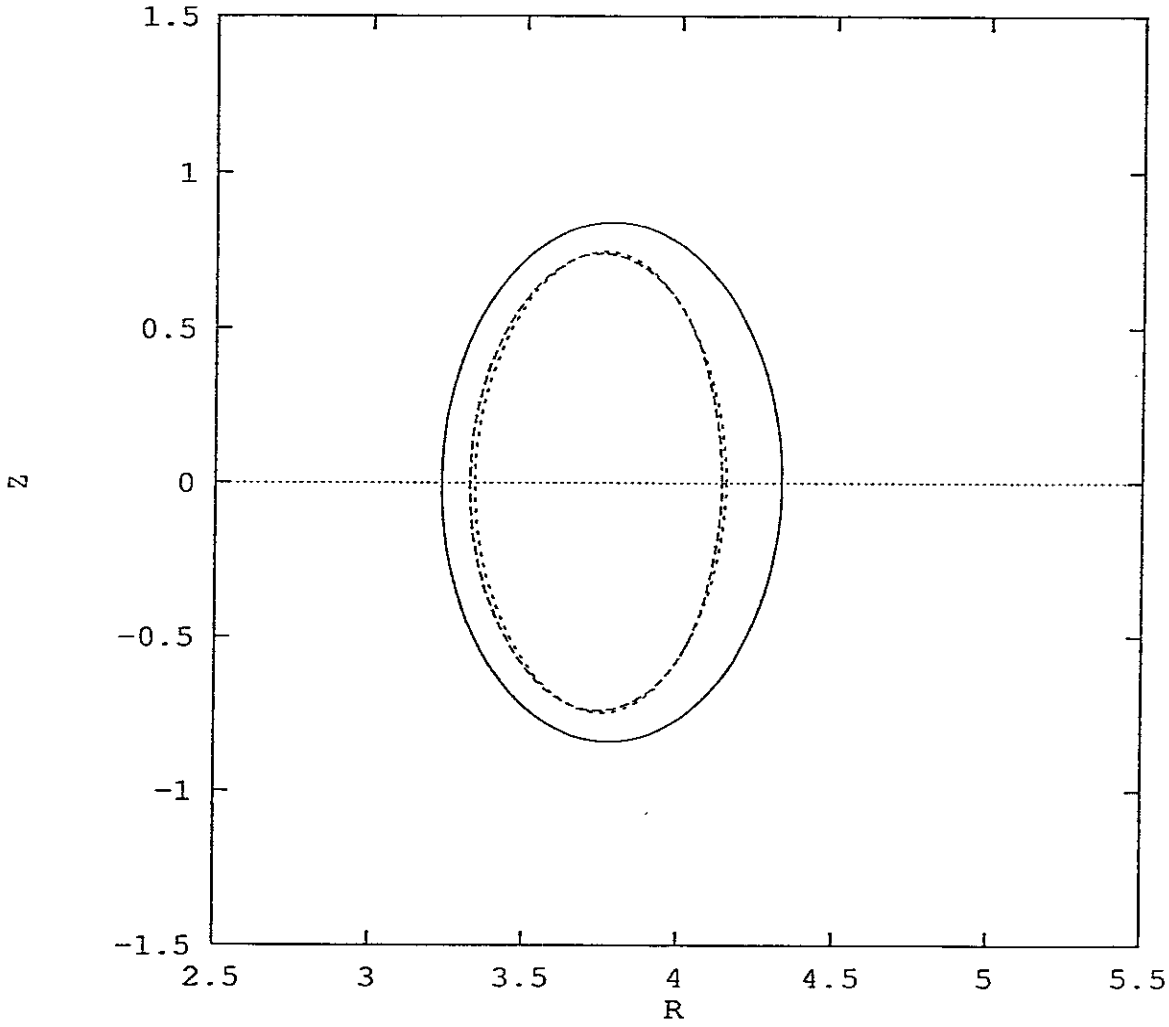

Figure 3: Bounding flux surfaces at $<\beta> = 0.14\%$ and $<\beta> = 2.7\%$ for Sequence 1 (broken lines) and the diamagnetic loop (solid line). In this cross-section, the higher $<\beta>$ equilibrium appears to be shifted inwards by the vertical field.

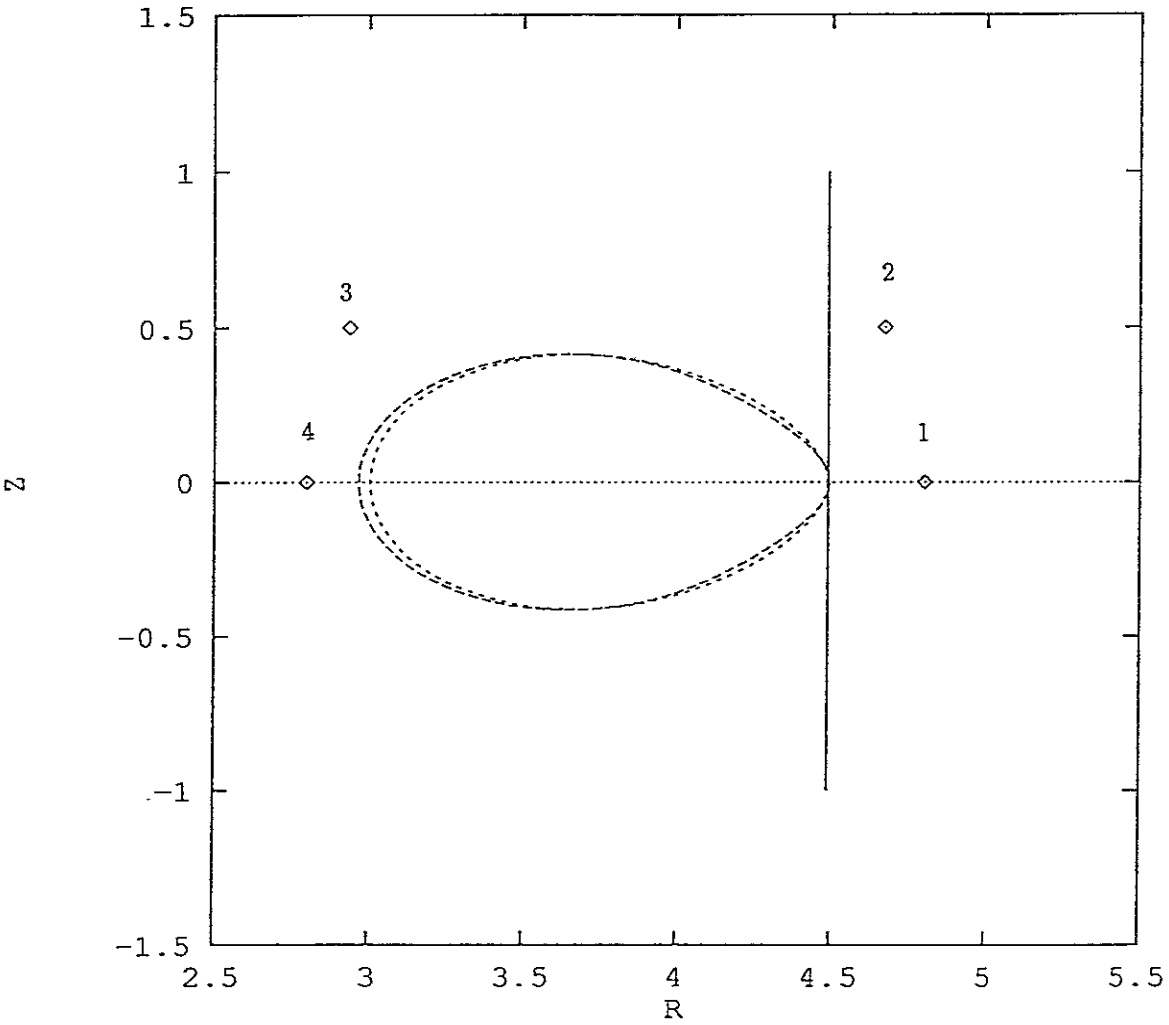

Figure 4: Bounding flux surfaces at $<\beta> = 0.14\%$ and $<\beta> = 2.7\%$ for Sequence 1 (broken lines), the limiter and the pick-up coils.

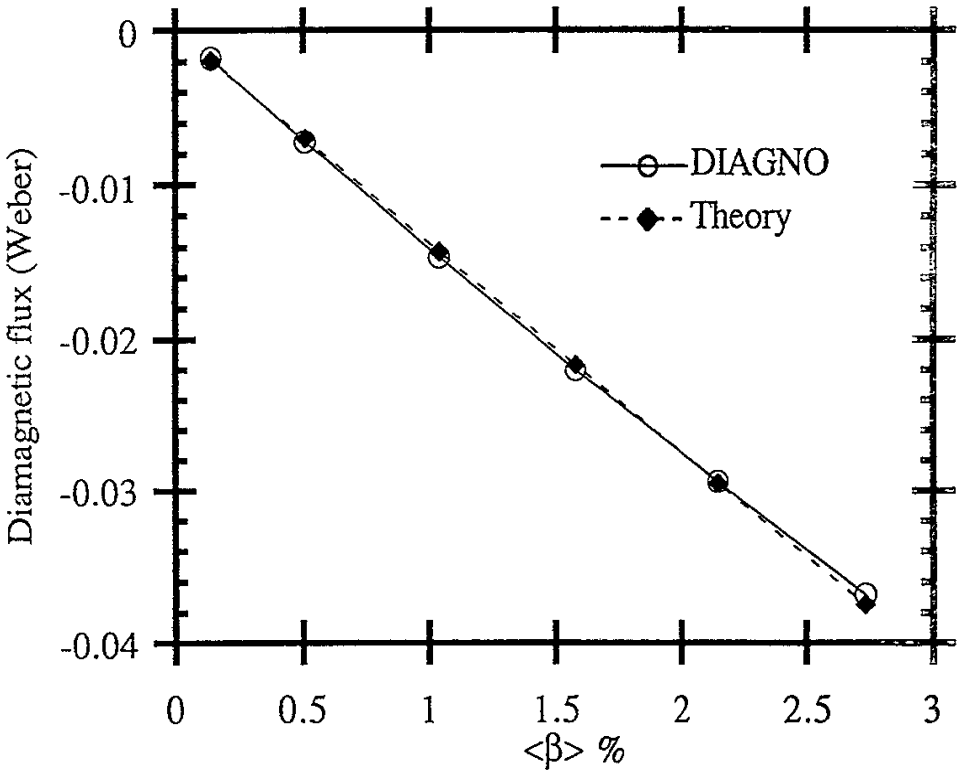

Figure 5: Diamagnetic flux compared with cylindrical theory for Sequence 1.

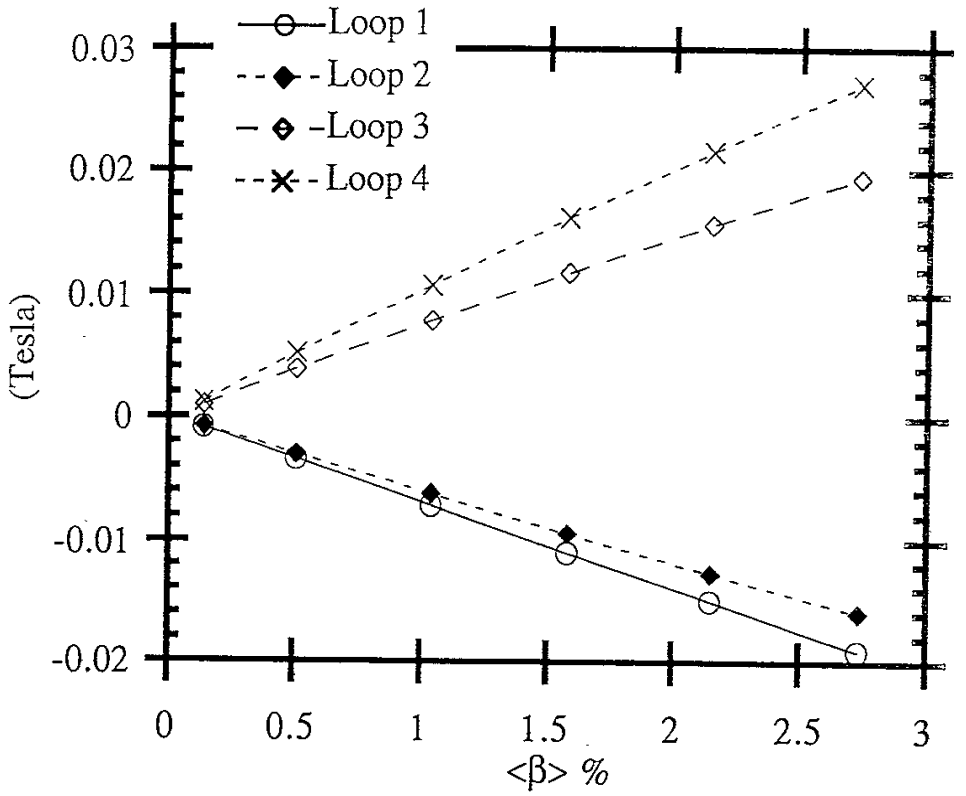

Figure 6: Signals expected at the pick-up loops for Sequence 1.

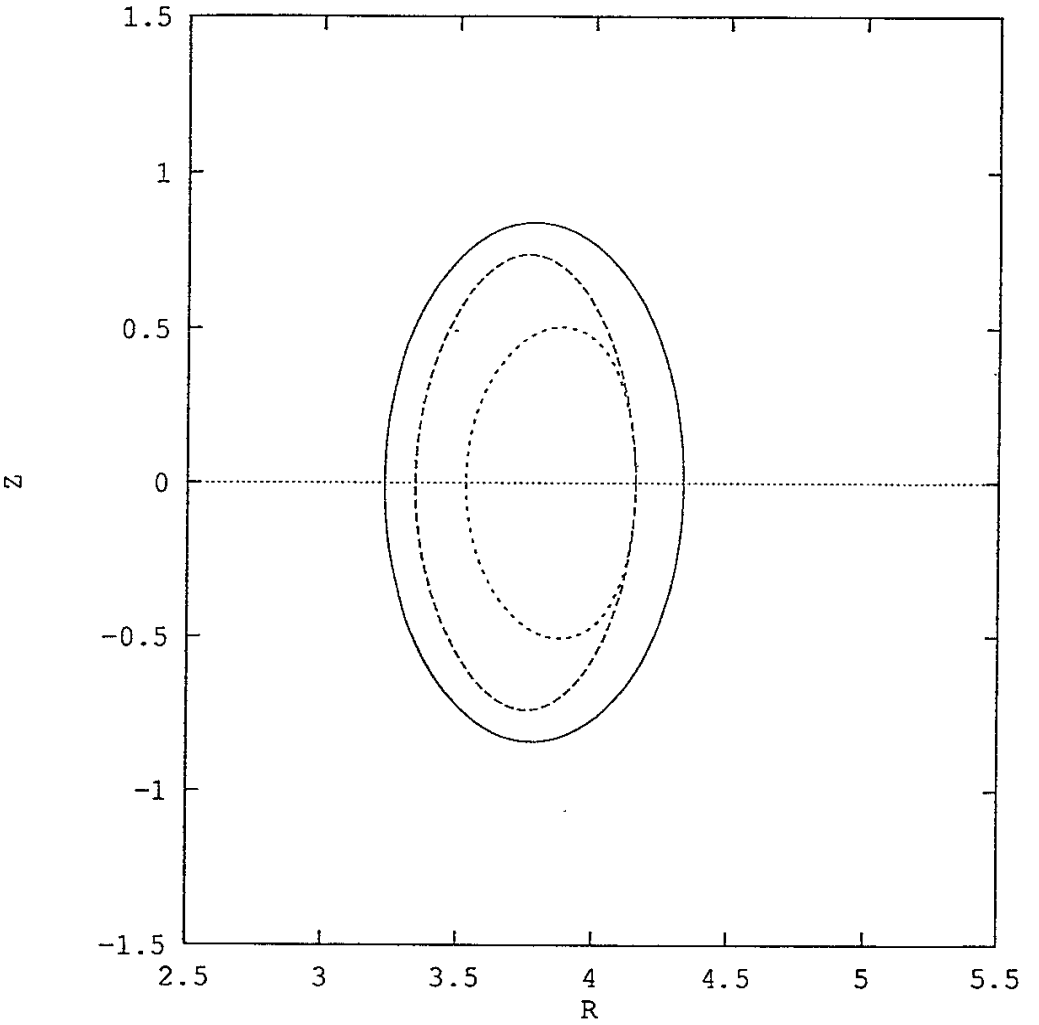

Figure 7: Bounding flux surfaces at $<\beta> = 0.14\%$ and $<\beta> = 3.0\%$ for Sequence 2 (broken lines) and the diamagnetic loop (solid line).

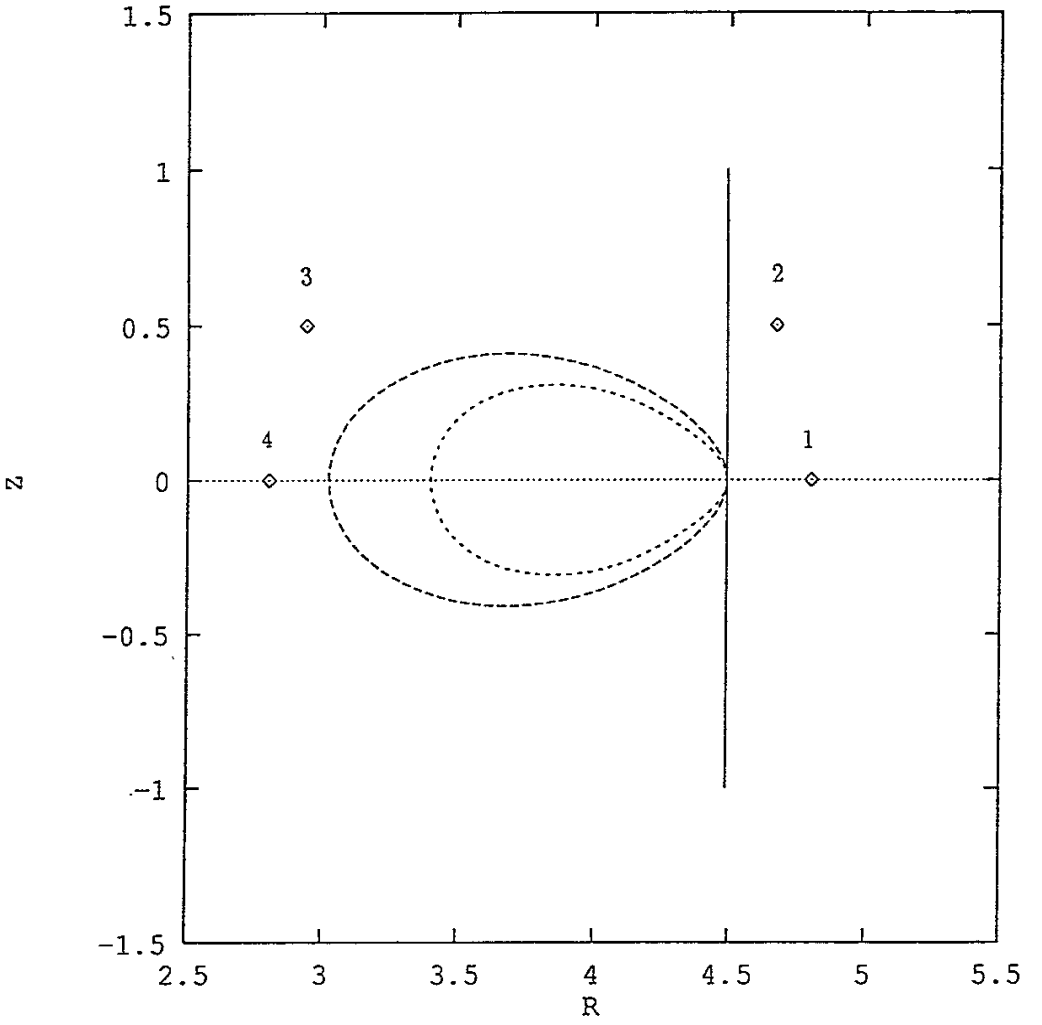

Figure 8: Bounding flux surfaces at $<\beta> = 0.14\%$ and $<\beta> = 3.0\%$ for Sequence 2 (broken lines), the limiter and the pick-up coils.

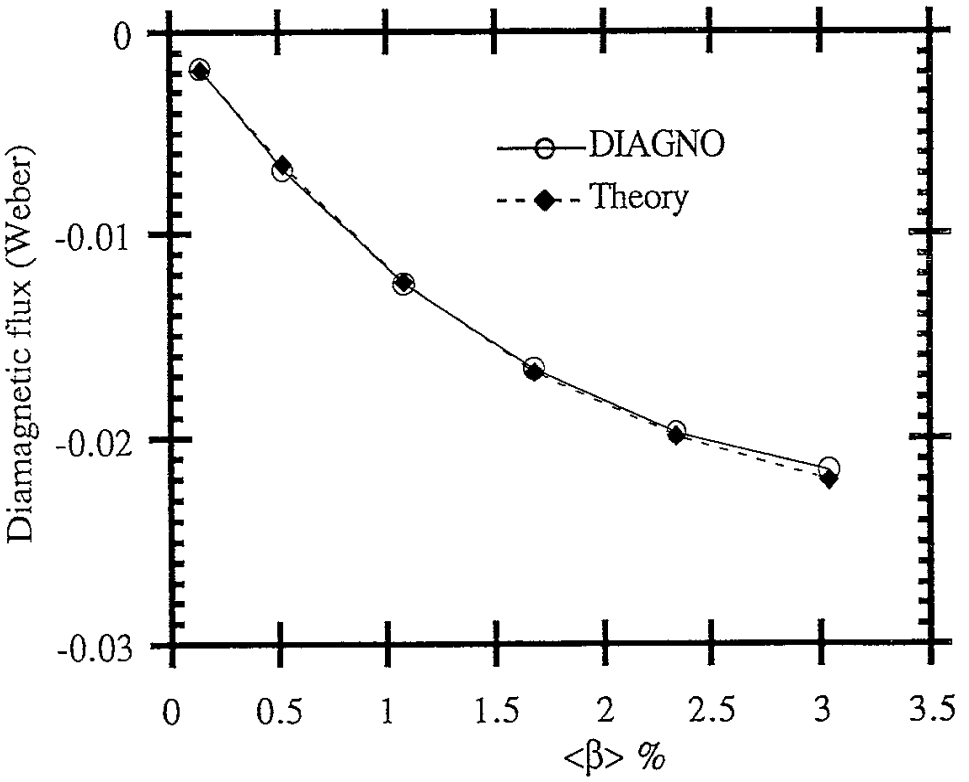

Figure 9: Diamagnetic flux compared with cylindrical theory for Sequence 2.

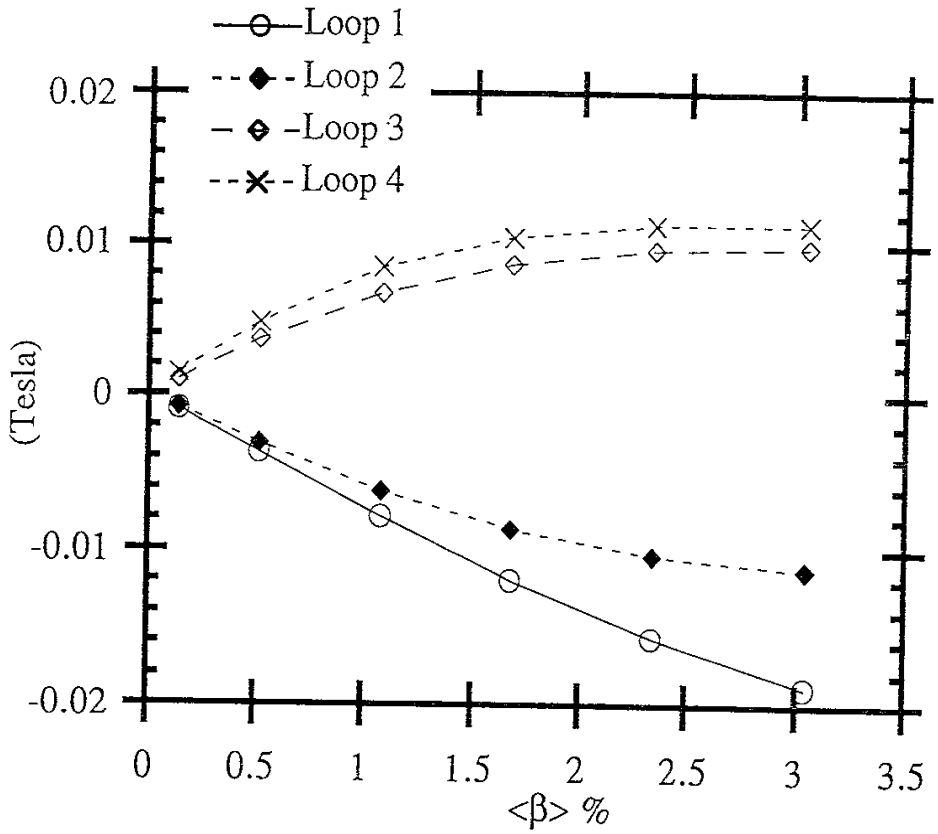

Figure 10: Signals expected at the pick-up loops for Sequence 2.

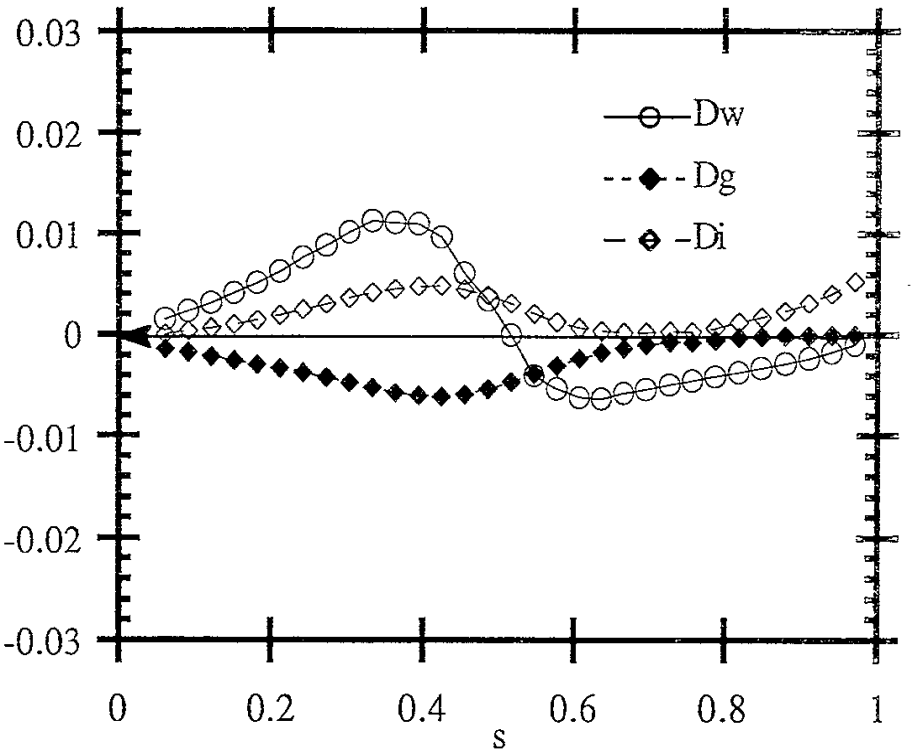

Figure 11: The "well", "current" and total ideal Mercier criterion for a Sequence 1 equilibrium at $<\beta> = 2.7\%$.

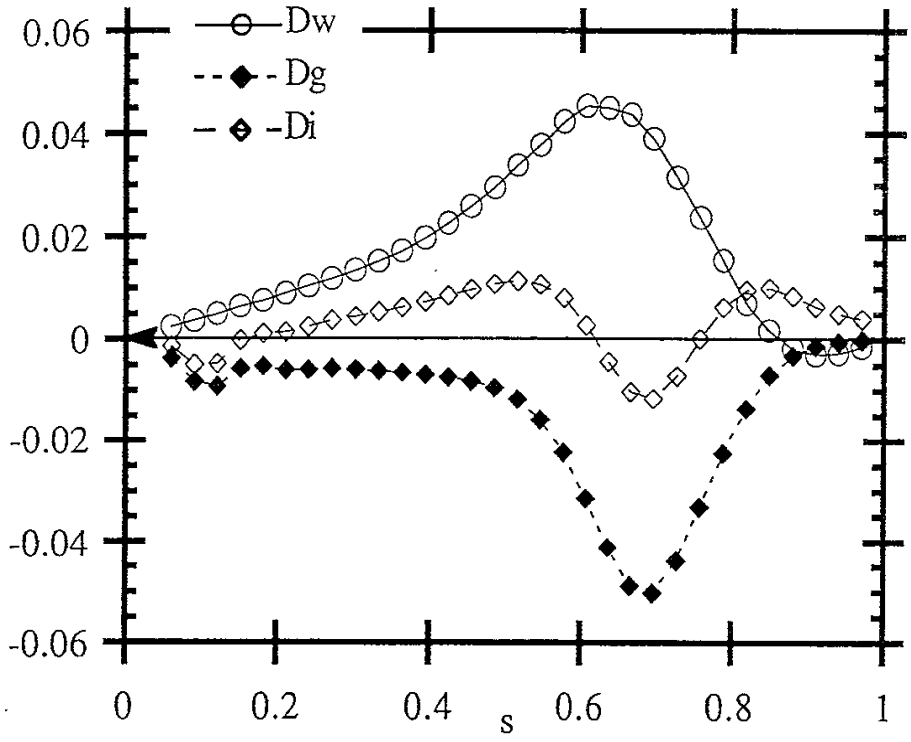

Figure 12: The "well", "current" and total ideal Mercier criterion for a Sequence 2 equilibrium at $<\beta>$ = 3.0%.

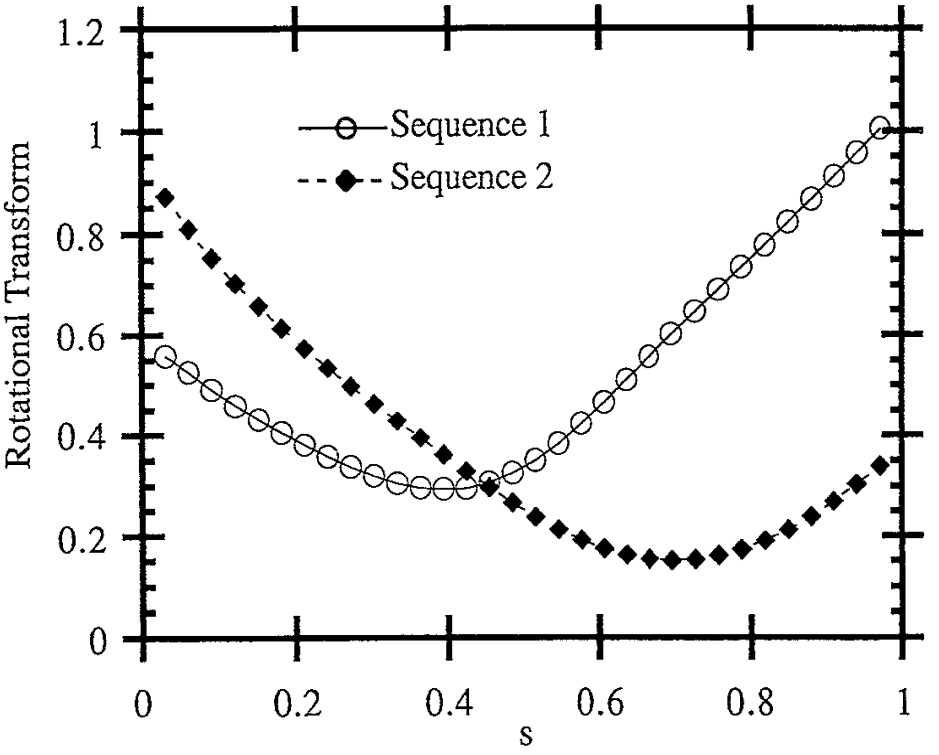

Figure 13: Rotational transform profiles for the equilibria of Figs. 11 and 12 against normalised flux.

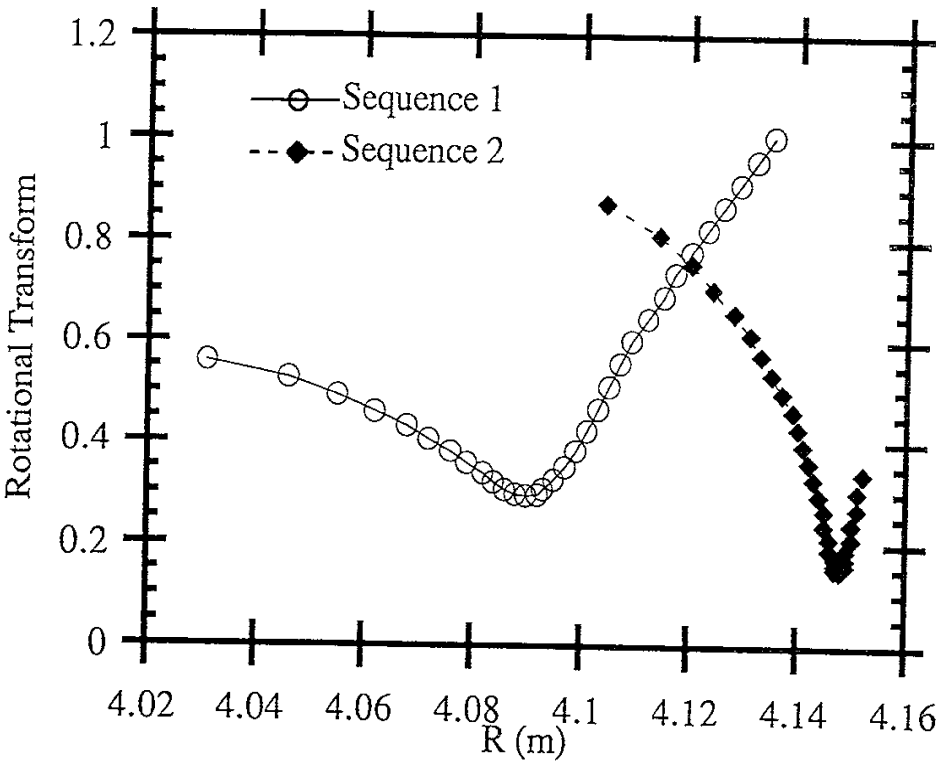

Figure 14: Rotational transform profiles for the equilibria of Figs. 11 and 12 against major radius in the cross-section of the vertical ellipse.

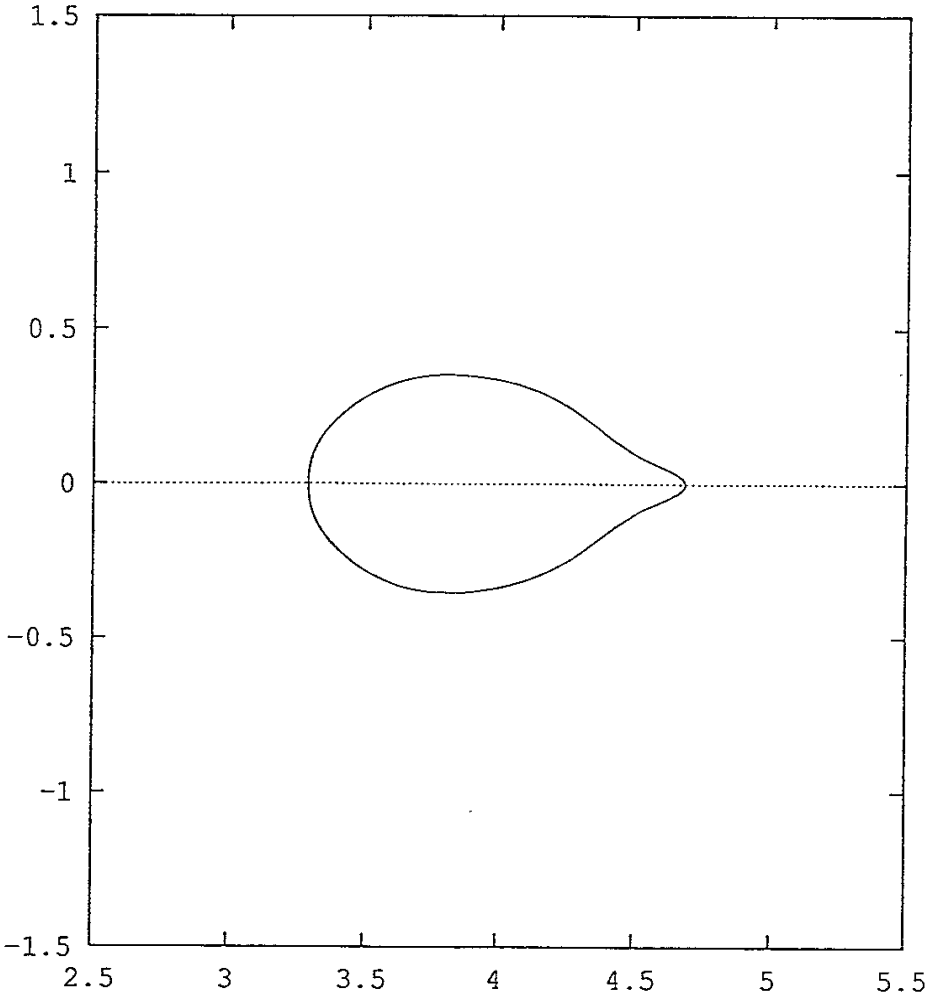

Figure 15: Cross-section of a free-boundary equilibrium which has attempted to pass through the separatrix.

Recent Issues of NIFS Series

NIFS-184 S. Okamura, K. Hanatani, K. Nishimura, R. Akiyama, T. Amano, H. Arimoto, M. Fujiwara, M. Hosokawa, K. Ida, H. Idei, H. Iguchi, O. Kaneko, T. Kawamoto, S. Kubo, R. Kumazawa, K. Matsuoka, S. Morita, O. Motojima, T. Mutoh, N. Nakajima, N. Noda, M. Okamoto, T. Ozaki, A. Sagara, S. Sakakibara, H. Sanuki, T. Seki, T. Shoji, F. Shimbo, C. Takahashi, Y. Takeiri, Y. Takita, K. Toi, K. Tsumori, M. Ueda, T. Watari, H. Yamada and I. Yamada, *Heating Experiments Using Neutral Beams with Variable Injection Angle and ICRF Waves in CHS* ; Sep. 1992

NIFS-185 H. Yamada, S. Morita, K. Ida, S. Okamura, H. Iguchi, S. Sakakibara, K. Nishimura, R. Akiyama, H. Arimoto, M. Fujiwara, K. Hanatani, S. P. Hirshman, K. Ichiguchi, H. Idei, O. Kaneko, T. Kawamoto, S. Kubo, D. K. Lee, K. Matsuoka, O, Motojima, T. Ozaki, V. D. Pustovitov, A. Sagara, H. Sanuki, T. Shoji, C. Takahashi, Y. Takeiri, Y. Takita, S. Tanahashi, J. Todoroki, K. Toi, K. Tsumori, M. Ueda and I. Yamada, *MHD and Confinement Characteristics in the High-β Regime on the CHS Low-Aspect-Ratio Heliotron / Torsatron* ; Sep. 1992

NIFS-186 S. Morita, H. Yamada, H. Iguchi, K. Adati, R. Akiyama, H. Arimoto, M. Fujiwara, Y. Hamada, K. Ida, H. Idei, O. Kaneko, K. Kawahata, T. Kawamoto, S. Kubo, R. Kumazawa, K. Matsuoka, T. Morisaki, K. Nishimura, S. Okamura, T. Ozaki, T. Seki, M. Sakurai, S, Sakakibara, A. Sagara, C. Takahashi, Y. Takeiri, H. Takenaga, Y. Takita, K. Toi, K. Tsumori, K. Uchino, M. Ueda, T. Watari, I. Yamada, *A Role of Neutral Hydrogen in CHS Plasmas with Reheat and Collapse and Comparison with JIPP T-IIU Tokamak Plasmas* ; Sep. 1992

NIFS-187 K. Ioth, S.-I. Itoh, A. Fukuyama, M. Yagi and M. Azumi, *Model of the L-Mode Confinement in Tokamaks* ; Sep. 1992

NIFS-188 K. Itoh, A. Fukuyama and S.-I. Itoh, *Beta-Limiting Phenomena in High-Aspect-Ratio Toroidal Helical Plasmas*; Oct. 1992

NIFS-189 K. Itoh, S. -I. Itoh and A. Fukuyama, *Cross Field Ion Motion at Sawtooth Crash* ; Oct. 1992

NIFS-190 N. Noda, Y. Kubota, A. Sagara, N. Ohyabu, K. Akaishi, H. Ji, O. Motojima, M. Hashiba, I. Fujita, T. Hino, T. Yamashina, T. Matsuda, T. Sogabe, T. Matsumoto, K. Kuroda, S. Yamazaki, H. Ise, J. Adachi and T. Suzuki, *Design Study on Divertor Plates of Large Helical Device (LHD)* ; Oct. 1992

NIFS-191 Y. Kondoh, Y. Hosaka and K. Ishii, *Kernel Optimum Nearly-Analytical*

Discretization (KOND) Algorithm Applied to Parabolic and Hyperbolic Equations : Oct. 1992

NIFS-192 K. Itoh, M. Yagi, S.-I. Itoh, A. Fukuyama and M. Azumi, *L-Mode Confinement Model Based on Transport-MHD Theory in Tokamaks* ; Oct. 1992

NIFS-193 T. Watari, *Review of Japanese Results on Heating and Current Drive* ; Oct. 1992

NIFS-194 Y. Kondoh, *Eigenfunction for Dissipative Dynamics Operator and Attractor of Dissipative Structure* ; Oct. 1992

NIFS-195 T. Watanabe, H. Oya, K. Watanabe and T. Sato, *Comprehensive Simulation Study on Local and Global Development of Auroral Arcs and Field-Aligned Potentials* ; Oct. 1992

NIFS-196 T. Mori, K. Akaishi, Y. Kubota, O. Motojima, M. Mushiaki, Y. Funato and Y. Hanaoka, *Pumping Experiment of Water on B and LaB_6 Films with Electron Beam Evaporator* ; Oct., 1992

NIFS-197 T. Kato and K. Masai, *X-ray Spectra from Hinotori Satellite and Suprathermal Electrons* ; Oct. 1992

NIFS-198 K. Toi, S. Okamura, H. Iguchi, H. Yamada, S. Morita, S. Sakakibara, K. Ida, K. Nishimura, K. Matsuoka, R. Akiyama, H. Arimoto, M. Fujiwara, M. Hosokawa, H. Idei, O. Kaneko, S. Kubo, A. Sagara, C. Takahashi, Y. Takeiri, Y. Takita, K. Tsumori, I. Yamada and H. Zushi, *Formation of H-mode Like Transport Barrier in the CHS Heliotron / Torsatron* ; Oct. 1992

NIFS-199 M. Tanaka, *A Kinetic Simulation of Low-Frequency Electromagnetic Phenomena in Inhomogeneous Plasmas of Three-Dimensions* ; Nov. 1992

NIFS-200 K. Itoh, S.-I. Itoh, H. Sanuki and A. Fukuyama, *Roles of Electric Field on Toroidal Magnetic Confinement*, Nov. 1992

NIFS-201 G. Gnudi and T. Hatori, *Hamiltonian for the Toroidal Helical Magnetic Field Lines in the Vacuum*; Nov. 1992

NIFS-202 K. Itoh, S.-I. Itoh and A. Fukuyama, *Physics of Transport Phenomena in Magnetic Confinement Plasmas*; Dec. 1992

NIFS-203 Y. Hamada, Y. Kawasumi, H. Iguchi, A. Fujisawa, Y. Abe and M. Takahashi, *Mesh Effect in a Parallel Plate Analyzer*; Dec. 1992

NIFS-204 T. Okada and H. Tazawa, *Two-Stream Instability for a Light Ion Beam*

-Plasma System with External Magnetic Field; Dec. 1992

NIFS-205 M. Osakabe, S. Itoh, Y. Gotoh, M. Sasao and J. Fujita, *A Compact Neutron Counter Telescope with Thick Radiator (Cotetra) for Fusion Experiment*; Jan. 1993

NIFS-206 T. Yabe and F. Xiao, *Tracking Sharp Interface of Two Fluids by the CIP (Cubic-Interpolated Propagation) Scheme*, Jan. 1993

NIFS-207 A. Kageyama, K. Watanabe and T. Sato, *Simulation Study of MHD Dynamo : Convection in a Rotating Spherical Shell*; Feb. 1993

NIFS-208 M. Okamoto and S. Murakami, *Plasma Heating in Toroidal Systems*; Feb. 1993

NIFS-209 K. Masai, *Density Dependence of Line Intensities and Application to Plasma Diagnostics*; Feb. 1993

NIFS-210 K. Ohkubo, M. Hosokawa, S. Kubo, M. Sato, Y. Takita and T. Kuroda, *R&D of Transmission Lines for ECH System* ; Feb. 1993

NIFS-211 A. A. Shishkin, K. Y. Watanabe, K. Yamazaki, O. Motojima, D. L. Grekov, M. S. Smirnova and A. V. Zolotukhin, *Some Features of Particle Orbit Behavior in LHD Configurations*; Mar. 1993

NIFS-212 Y. Kondoh, Y. Hosaka and J.-L. Liang, *Demonstration for Novel Self-organization Theory by Three-Dimensional Magnetohydrodynamic Simulation*; Mar. 1993

NIFS-213 K. Itoh, H. Sanuki and S.-I. Itoh, *Thermal and Electric Oscillation Driven by Orbit Loss in Helical Systems*; Mar. 1993

NIFS-214 T. Yamagishi, *Effect of Continuous Eigenvalue Spectrum on Plasma Transport in Toroidal Systems*; Mar. 1993

NIFS-215 K. Ida, K. Itoh, S.-I.Itoh, Y. Miura, JFT-2M Group and A. Fukuyama, *Thickness of the Layer of Strong Radial Electric Field in JFT-2M H-mode Plasmas*; Apr. 1993

NIFS-216 M. Yagi, K. Itoh, S.-I. Itoh, A. Fukuyama and M. Azumi, *Analysis of Current Diffusive Ballooning Mode*; Apr. 1993

NIFS-217 J. Guasp, K. Yamazaki and O. Motojima, *Particle Orbit Analysis for LHD Helical Axis Configurations* ; Apr. 1993

NIFS-218 T. Yabe, T. Ito and M. Okazaki, *Holography Machine HORN-1 for Computer-aided Retrieve of Virtual Three-dimensional Image* ; Apr. 1993

NIFS-219 K. Itoh, S.-I. Itoh, A. Fukuyama, M. Yagi and M. Azumi, *Self-sustained Turbulence and L-Mode Confinement in Toroidal Plasmas* ; Apr. 1993

NIFS-220 T. Watari, R. Kumazawa, T. Mutoh, T. Seki, K. Nishimura and F. Shimpo, *Applications of Non-resonant RF Forces to Improvement of Tokamak Reactor Performances Part I: Application of Ponderomotive Force* ; May 1993

NIFS-221 S.-I. Itoh, K. Itoh, and A. Fukuyama, *ELMy-H mode as Limit Cycle and Transient Responses of H-modes in Tokamaks* ; May 1993

NIFS-222 H. Hojo, M. Inutake, M. Ichimura, R. Katsumata and T. Watanabe, *Interchange Stability Criteria for Anisotropic Central-Cell Plasmas in the Tandem Mirror GAMMA 10 ;* May 1993

NIFS-223 K. Itoh, S.-I. Itoh, M. Yagi, A. Fukuyama and M. Azumi, *Theory of Pseudo-Classical Confinement and Transmutation to L-Mode;* May 1993

NIFS-224 M. Tanaka, *HIDENEK: An Implicit Particle Simulation of Kinetic-MHD Phenomena in Three-Dimensional Plasmas;* May 1993

NIFS-225 H. Hojo and T. Hatori, *Bounce Resonance Heating and Transport in a Magnetic Mirror;* May 1993

NIFS-226 S.-I. Iton, K. Itoh, A. Fukuyama, M. Yagi, *Theory of Anomalous Transport in H-Mode Plasmas;* May 1993

NIFS-227 T. Yamagishi, *Anomalous Cross Field Flux in CHS ;* May 1993

NIFS-228 Y. Ohkouchi, S. Sasaki, S. Takamura, T. Kato, *Effective Emission and Ionization Rate Coefficients of Atomic Carbons in Plasmas;* June 1993

NIFS-229 K. Itoh, M. Yagi, A. Fukuyama, S.-I. Itoh and M. Azumi, *Comment on 'A Mean Field Ohm's Law for Collisionless Plasmas;* June 1993

NIFS-230 H. Idei, K. Ida, H. Sanuki, H. Yamada, H. Iguchi, S. Kubo, R. Akiyama, H. Arimoto, M. Fujiwara, M. Hosokawa, K. Matsuoka, S. Morita, K. Nishimura, K. Ohkubo, S. Okamura, S. Sakakibara, C. Takahashi, Y. Takita, K. Tsumori and I. Yamada, *Transition of Radial Electric Field by Electron Cyclotron Heating in Stellarator Plasmas;* June 1993